

This manuscript analyzed 3 months continuous measurement of particle size distribution from 1.2 nm to 10000 nm during winter 2018 in Beijing. This kind of observation, that cover almost the full range of particle size and include both charged and neutral clusters/particles, is rather limited in China. New particle formation and haze days were discussed separately, and found a clear correlation between the cluster and nucleation modes during NPF days. In addition, the work found that all modes in the sub-micron size range were correlated with NO_x, indicate traffic emission can contribute to all particle sizes. In general, the manuscript did provide useful information and knowledge, but some more in-depth analysis is encouraged. The manuscript is in general well written and documented. The topic fits well in the scope of ACP. I recommend this manuscript can be published after some revisions.

We would like to thank the referee for the suggestions and careful editorial comments. Our replies (text in blue) to the comments (text in black) item by item and modification in our manuscript (text in red) as per suggestions of the referee are presented as below:

Comments:

More discussions on the charged ions/clusters from NAIS are encouraged. Can the ion induced nucleation be observed? Is it important?

We thank the reviewer for their suggestions. We did observe ion induced nucleation during our observation however we think that it constitutes only a minor fraction in comparison to neutral nucleation mechanism. Both cluster ion number concentration and the formation rate of 1.5 nm ions constituted a small fraction of total clusters number concentration and total formation rate of 1.5 nm clusters.

The following discussion and figures (Figure R1-1, Figure R1-2, Figure R1-3 and Figure R1-4) were added to the manuscript:

2.4.1 Calculation of the growth rate

The growth rates of cluster and nucleation mode particles were calculated from positive ion data and particle data from Neutral Cluster and Air Ion Spectrometer (NAIS), respectively, by using the appearance time method introduced by Lehtipalo et al. (2014). In this method, the particle number concentration of particles of size dp is recorded as a function of time, and the appearance time of particles of size dp is determined as the time when their number concentration reaches 50% of its maximum value during new particle formation (NPF) events.

The growth rates (GR) were calculated according to:

$$GR = \frac{dp_2 - dp_1}{t_2 - t_1} \quad (1)$$

where t_2 and t_1 are the appearance times of particles with sizes of dp_2 and dp_1 respectively. Figure R1-4 shows an example of how this method was used.

2.4.2 Calculation of the coagulation sink

The coagulation sink (CoagS) was calculated according to the equation (2) introduced by Kulmala et al. (2012):

$$CoagS_{dp} = \int K(dp, d'p)n(d'p)dd'p \cong \sum_{d'p=dp}^{d'p=max} K(dp, d'p)N_{d'p} \quad (2)$$

where $K(dp, d'p)$ is the coagulation coefficient of particles with sizes of dp and $d'p$, $N_{d'p}$ is the particle number concentration with size of $d'p$.

2.4.3 Calculation of the formation rate

The formation rate of 1.5-nm particles ($J_{1.5}$) was calculated using particle number concentrations measured with a Particle Sizer Magnifier (PSM). The formation rate of 1.5-nm ions ($J_{1.5}^{\pm}$) was calculated using positive and negative ions data from the Neutral Cluster and Air Ion Spectrometer (NAIS) as well as PSM data. The upper limit used was 3 nm. The values of $J_{1.5}$ and $J_{1.5}^{\pm}$ were calculated following the methods introduced by Kulmala et al. (2012) with equation (3) and equation (4), respectively:

$$J_{dp} = \frac{dN_{dp}}{dt} + CoagS_{dp} \cdot N_{dp} + \frac{GR}{\Delta dp} \cdot N_{dp} \quad (3)$$

where $CoagS_{dp}$ is coagulation sink in the size range of $[dp, dp + \Delta dp]$ and GR is the growth rate.

$$J_{dp}^{\pm} = \frac{dN_{dp}^{\pm}}{dt} + CoagS_{dp} \cdot N_{dp}^{\pm} + \frac{GR}{\Delta dp} \cdot N_{dp}^{\pm} + \alpha \cdot N_{dp}^{\pm} \cdot N_{<dp}^{\mp} - \chi N_{dp} \cdot N_{<dp}^{\pm} \quad (4)$$

The fourth and fifth terms on the right hand side of equation (4) represent ion-ion recombination and charging of neutral particles by smaller ions, respectively, α is the ion-ion recombination coefficient and χ is the ion-aerosol attachment coefficient.

3.5 Atmospheric ions and ion induced nucleation in Beijing

In order to estimate the contribution of ions to the total cluster mode particle number concentration and the importance of ion induced nucleation in Beijing, we studied ion number concentrations in the size range of 0.8-7 nm by dividing them into 3 sub-size bins: constant pool (0.8-1.5 nm), charged clusters (1.5-3 nm) and larger ions (3-7 nm). As shown in Figure R1-1, number concentrations of positive ions were higher than those negative ions in all the size bins on both NPF event days and haze days. We will only discuss positive ions here.

The median number concentration of positive ions in the constant pool on NPF event days was only 100 cm^{-3} in Beijing, much less than that in boreal forest (600 cm^{-3} ; Mazon et al., 2016). Also, the median number concentration of positive charged clusters was 20 cm^{-3} on the NPF event days, and the ratio to the total cluster mode particle number concentration was 0.001 to 0.004 during the NPF time window (Figure R1-2). This ratio is comparable to that observed in San Pietro Capofiume (0.004), in which the anthropogenic pollution level was also high, but clearly lower than that observed in another megacity in China, Nanjing, (0.02) (Kontkanen et al., 2017). Considerably higher ratios were observed in clean environments, for example during winter in the boreal forest at Hyytiälä, Finland (0.7; Kontkanen et al., 2017). The median number concentration of larger ions (3- 7 nm) on the NPF event days was 30 cm^{-3} , a little bit

higher than the charged cluster mode particle number concentration, indicating that not all of the larger ions originate from the growth of charged clusters, but rather from charging of neutral particles by smaller ions. On the haze days, charged ion number concentrations were much lower than those on the NPF days which could be attributed to the higher condensation sink.

The diurnal pattern of the ratio of number concentration between charged and total cluster mode particles was the highest during the night with a maximum of 0.008, and had a trough during daytime with a minimum of 0.001 on the NPF event days. Such diurnal pattern is similar to earlier observations in Nanjing, San Pietro Capofiume and Hyytiälä (Kontkanen et al., 2017). This ratio reached its minimum around noon, because the total cluster mode particle number concentration reached its maximum around that time due to NPF. The ratio had a small peak at around 9:00, similar to earlier observations in Centreville and Po Valley (Kontkanen et al., 2016; Kontkanen et al., 2017). The possible reason is that charged clusters were activated earlier in the morning than neutral clusters. The ratio increased from the midnight until about 4:00, similar to the number concentration of charged clusters.

As shown in Figure R1-3, the diurnal median of the ratio between the formation rate of positive ions of 1.5 nm ($J_{1.5}^+$) and the total clusters of 1.5 nm ($J_{1.5}$) varied from 0.0009 to 0.006. This result is comparable to observations in Shanghai, where the positive ion induced nucleation contributed only 0.05% to the total formation rate of 1.7-nm particles ($J_{1.7}$) (Yao et al., 2018).

There are some overlap for the particle size distribution between NAIS and PSD. It would be good that the authors can provide some information about the inter comparison between these two techniques.

Indeed, we added the discussion on instrument comparison and related figures (Figure R1-5 and Figure R1-6) to the manuscript (line 186) as per suggestion of the referee.

The Particle Size Distribution system (PSD) and Neutral Cluster and Air Ion Spectrometer (NAIS) had an overlapping particle size distribution over the mobility diameter range of 3-42 nm. As shown in Figure R1-5, total particle number concentrations from the NAIS and PSD system correlated well with each other on both NPF event days (R^2 was 0.92) and haze days (R^2 was 0.90) in the overlapping size range. The slopes between the total particle number concentration from the PSD system and that from the NAIS were 0.90 and 0.85 on the NPF event days and haze days, respectively. The particle number size distribution in the overlapping size range of the NAIS and PSD system matched well on both NPF event days and haze days as shown in Figure R1-6.

I would suggest to provide 1 plot to show the traffic emission derived increase of cluster and nucleation mode particles, and maybe the correlation plot between cluster mode particles and NO_x during the non-NPF days.

We thank the referee for the suggestions. We added Figure R1-7 to the manuscript. Correspondingly, we updated our discussion in lines 252- 259 as below:

In Figure R1-7, we show the median diurnal pattern of particle number size distribution on the NPF event days and haze days separately. On the NPF event days, we observed cluster formation from diameters smaller than 3 nm. The growth of newly-formed particles lasted for

several hours, resulting in a consecutive increase of the particle number concentrations in all the four modes. During traffic rush hours in the morning and evening, we observed an increase of particle number concentrations in the size range of cluster mode to around 100 nm.

On the haze days, we still observed an increase of particle number concentration in the size range of cluster mode to Aitken mode during rush hours. Traditionally, NPF events occur during the time window between sunrise and sunset by photochemical reactions (Kerminen et al., 2018). The binary or ternary nucleation between sulfuric acid and water, ammonia or amines are usually thought of as sources of atmospheric cluster mode particles, especially in heavily polluted environments (Kulmala et al., 2013; Kulmala et al., 2014; Yao et al., 2018; Chu et al., 2019). The burst of cluster mode particle number concentration outside the traditional NPF time window, especially during the rush hours in the afternoon, suggests a very different source of cluster mode particles from traditional nucleation, e.g. nucleation from gases emitted by traffic (Rönkkö et al., 2017).

As shown in Figure 6, on the NPF event days, the cluster mode particle number concentration started to increase at the time of sunrise and peaked around noon with a wide single peak, showing the typical behavior related to NPF events (Kulmala et al., 2012). Comparatively, on the haze days, the cluster mode particle number concentration showed a double peak pattern similar to the diurnal cycle of NO_x (Figure 5). This observation is consistent with our discussion above that traffic emission possibly contributed to cluster mode particles. By comparing cluster mode particle number concentrations between the haze days and NPF event days, we estimated that traffic-related cluster mode particles could contribute up to 40-50 % of the total cluster mode particle number concentration on the NPF event days.

It is a bit unusual that there were no overlap between NPF and haze days. There were quite many studies that observed NPF with considerable high concentrations of $\text{PM}_{2.5}$. What will happen if classify the haze days by the concentration of $\text{PM}_{2.5}$, i.e. $100 \mu\text{g}/\text{m}^3$?

We thank the referee for the suggestions. We observed NPF events and haze events on the same days, but not at the same time. We classified haze days not only according to the visibility and relative humidity but also according to the time period haze events lasted. Days were classified as haze days when haze lasted for at least 12 consecutive hours. According to this classification, we did not observe any overlap between NPF event days and haze days.

As per suggestion to the referee, we classified haze days by the concentration of $\text{PM}_{2.5}$, i.e. $100 \mu\text{g}/\text{m}^3$. We show time series of particle number size distribution and $\text{PM}_{2.5}$ concentration during our observations in Figure R1-8. In Figure R1-8, the NPF events can be identified with the 'banana shapes'. We did not observe any NPF events happening at the same time when $\text{PM}_{2.5}$ concentration was higher than $100 \mu\text{g}/\text{m}^3$.

Table 2, change the color-marked numbers to, i.e. bold or italic.

We modified Table 2 as per suggestion to the referee.

Figs. 7-9, where were the data points of "others"?

The data points of 'others' are those that do not belong to the classification of NPF or haze days. They are usually polluted days during which we do not observe any NPF, but cannot be

classified as haze days due to low PM loading resulting in not so bad visibility. To make the plots clearer, we only present NPF and haze days here.

Fig. 9, there showed pretty good correlation between Aitken mode particles and accumulation mode particles during NPF days. What's the possible reason?

On the NPF event days, Aitken and accumulation mode particle number concentrations correlated positively with each other, as well as with the SO₂ and NO_x concentration. This suggests that on the NPF event days, Aitken and accumulation mode particles were both formed during regional transportation as secondary particles and were emitted by traffic as primary particles.

To make the discussion on correlation between each of the modes, we updated the discussion at section 3.4 and separate Table 3 into Table R1a and Table R1b according NPF event days and haze days, in addition we changed Figure 9 into Figure R1-9 as following:

3.4 Correlation between different particle modes

Table R1a and Table R1b as well as Figure R1-9 show the correlation between particle number concentrations in different modes. On the NPF event days, cluster and nucleation mode particle number concentrations correlated positively with each other due to their common dominant source, NPF. Both cluster and nucleation mode particle number concentrations correlated negatively with the Aitken and accumulation mode particle number concentrations because, as discussed earlier, high concentrations of large particles tend to suppress NPF and subsequent growth of newly-formed particles.

On the NPF event days, Aitken and accumulation mode particle number concentrations correlated positively with each other, as well as with the SO₂ and NO_x concentration. This suggests that on the NPF event days, Aitken and accumulation mode particles both formed during regional transportation as secondary particles and were emitted by traffic as primary particles.

On the haze days, cluster and nucleation mode particle number concentrations correlated positively with each other, and with the Aitken mode particle number concentration. This is suggestive of a similar dominating sources for these particle, most likely traffic emissions. Similar to the NPF event days, cluster and nucleation mode particle number concentrations correlated negatively with the accumulation mode particle number concentration, even though this correlation was rather weak (Table R1b).

The Aitken mode particle number concentration had a negative correlation with the accumulation mode particle number concentration on the haze days.

Figures and Tables

Table R1a: Correlation coefficients between particle number concentration of every mode on NPF event days. The time window was 08:00 - 14:00. High correlation coefficients ($|R|>0.5$) are marked with bold and italic.

	Cluster	Nucleation	Aitken	Accumulation
Cluster	1			
Nucleation	0.76 ^a	1		
Aitken	-0.46 ^a	-0.33 ^b	1	
Accumulation	-0.66 ^a	-0.66 ^c	0.7 ^c	1

^a included 516 data points (the time resolution was 12 minutes), ^b included 1251 data points (the time resolution was 5 min), ^c included 1331 data points (the time resolution was 5 min).

Table R1b: Correlation coefficients between particle number concentration of every mode on haze days. The time window was 08:00 - 14:00. High correlation coefficients ($|R|>0.5$) are marked with bold and italic.

	Cluster	Nucleation	Aitken	Accumulation
Cluster	1			
Nucleation	0.74 ^a	1		
Aitken	0.41 ^a	0.48 ^b	1	
Accumulation	-0.22 ^a	-0.33 ^c	-0.5 ^c	1

^a included 342 data points (the time resolution was 12 minutes), ^b included 824 data points (the time resolution was 5 min), ^c included 845 data points (the time resolution was 5 min).

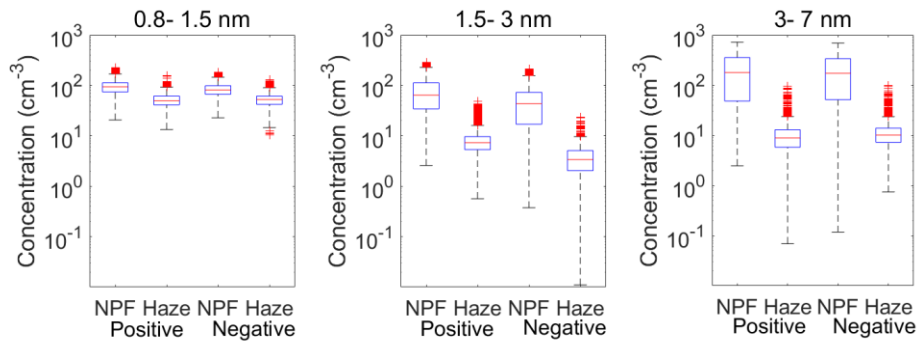


Figure R1-1: Positive and negative ion number concentrations in the size bins of 0.8- 1.5nm, 1.5-3 nm and 3-7 nm on NPF event days and haze days separately. The whiskers include 99.3% of data of every group. Data out of $1.5 \times$ interquartile range are posited outside the whiskers and considered as outliers. The lines in the boxes represent the median value, the lower of the boxes represent 25% of the number concentration, and the upper of the boxes represent 75% of the number concentration. Data marked with red pluses represent outliers.

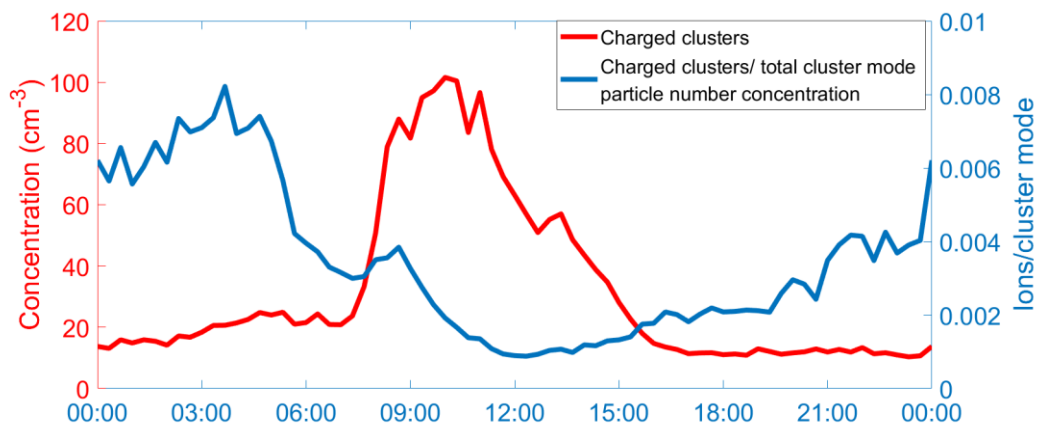


Figure R1-2: Diurnal pattern of charged clusters (1.5-3 nm) number concentration (red line) and ratio of charged clusters to total cluster mode (1.5-3 nm) particle number concentration on the NPF event days (blue line). The time resolution of the used data was 12 min.

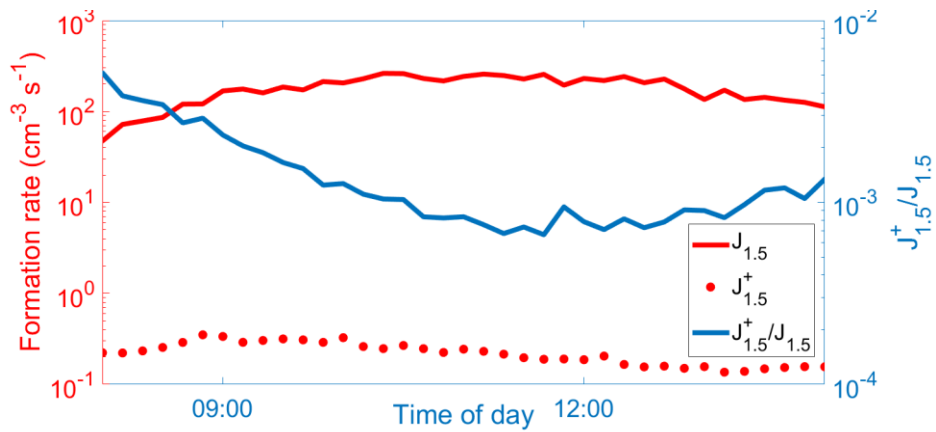


Figure R1-3: Diurnal pattern of formation rate of positive charged clusters of 1.5 nm (red dots) and neutral clusters of 1.5 nm (red line) and the ratio between them (blue line) on the NPF event days during the NPF time window we chose. The time resolution of the used data was 12 min.

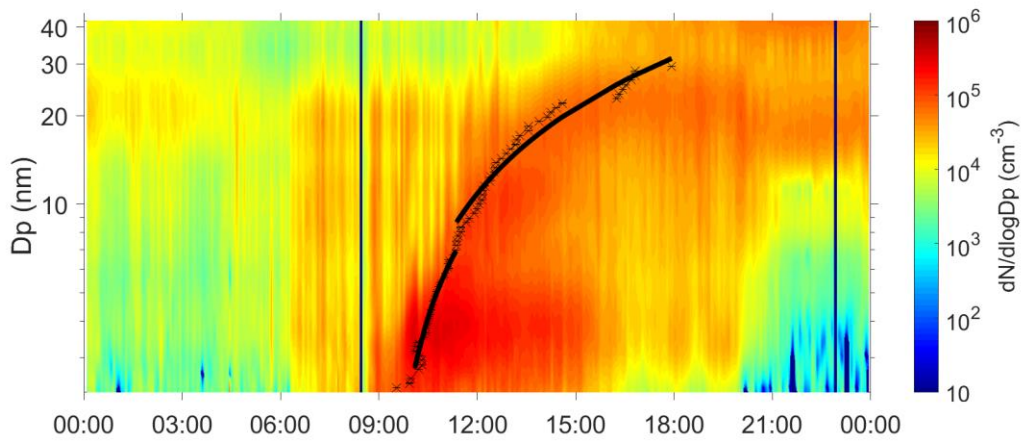


Figure R1-4: An example of how the appearance time method was used to calculate growth rate. The appearance time was recorded as a function of particle diameter as the black stars in the figure. The black lines are the fitted growth periods. The growth rates were calculated by calculating the slopes of the black lines.

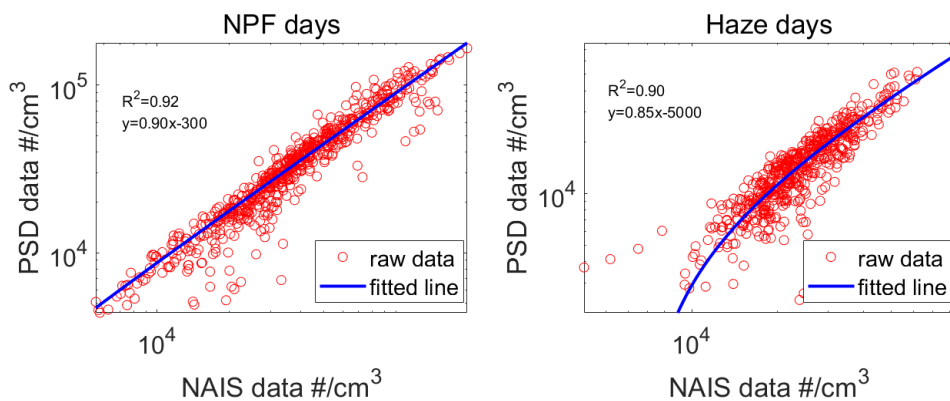


Figure R1-5: Total particle number concentration in size range of 3-42 nm from NAIS and PSD system. There are 1271 data points on the plots of NPF days and 887 data points on the plots of haze days. The time resolution was 5 minutes.

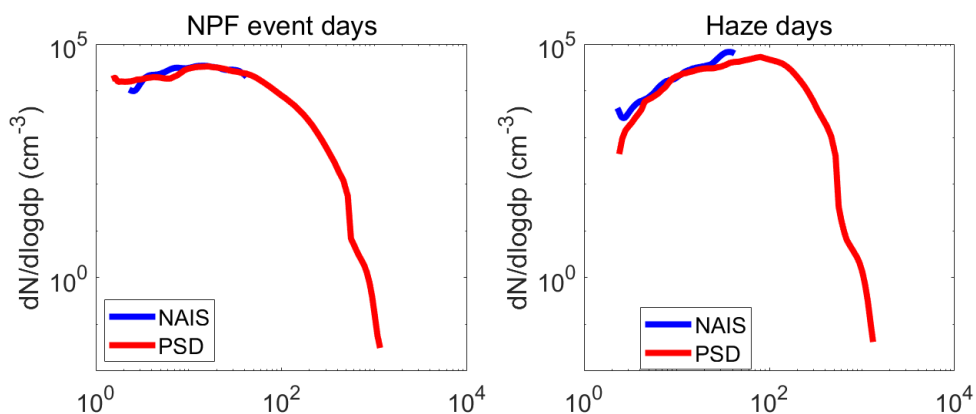


Figure R1-6: Median particle number size distribution of data from NAIS (blue line) and PSD system (red line) on NPF event days (left panel) and haze days (right panel) during our observation. The time resolution we used here for every point was 1h.

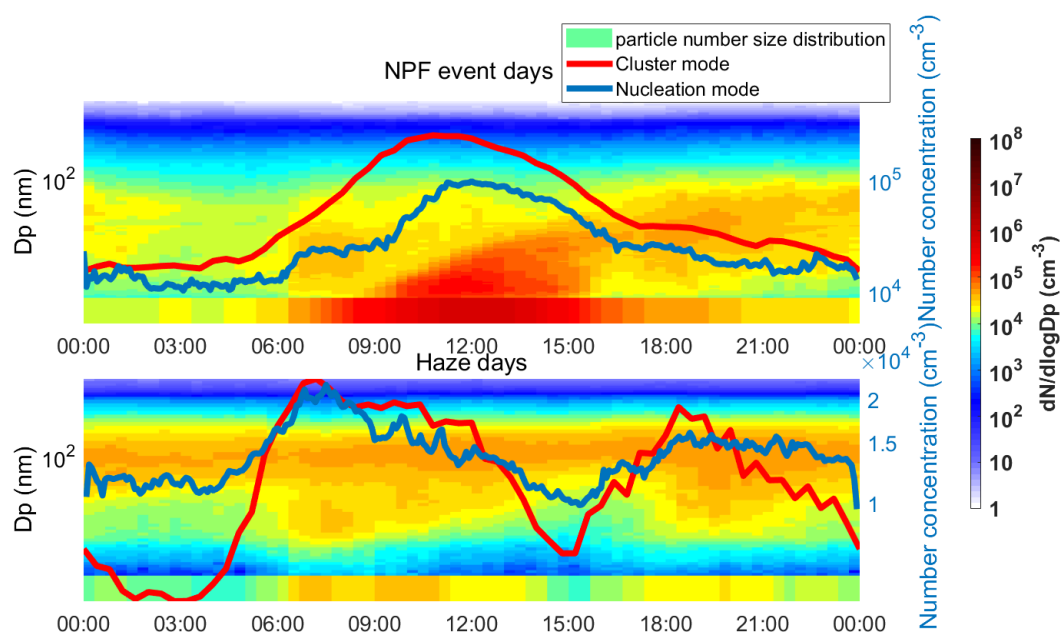


Figure R1-7: Median diurnal patterns of the particle number size distribution over the size range of 1.5-1000 nm and number concentrations of cluster mode (red lines) and nucleation mode (blue lines) particles on the NPF event days (upper panel) and haze days (lower panel). The time resolution for every data point of particle number size distribution and cluster mode particle number concentration was 12 minutes. The time resolution of every data point of nucleation mode particle number concentration was 5 minutes.

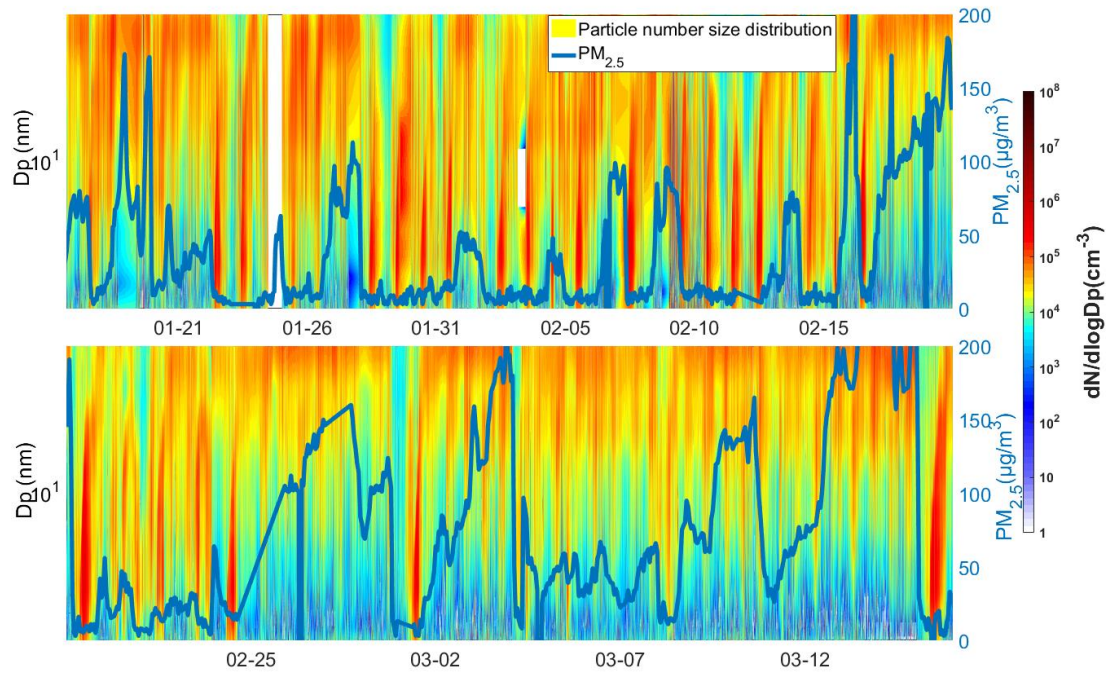


Figure R1-8: Time series of particle number size distribution and $PM_{2.5}$ concentration (blue line) during our observation period.

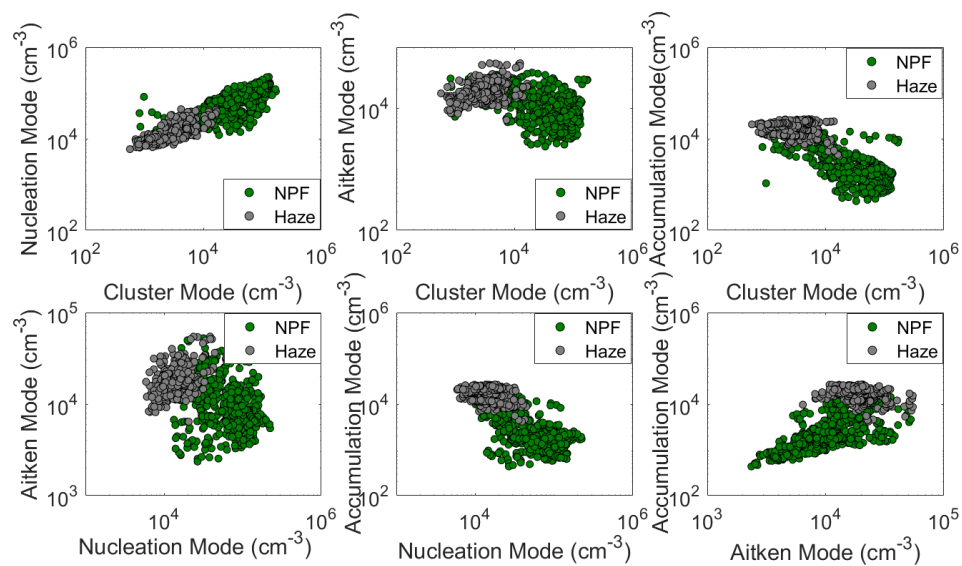


Figure R1-9: Correlation between every mode each other on NPF event days (green dots) and haze days (grey dots). The time resolution of data in the plots of correlation between cluster mode and other modes was 12 min and the time resolution of other data points was 5 min.

References

- Chu, B. W., Kerminen, V. M., Bianchi, F., Yan, C., Petäjä, T., and Kulmala, M.: Atmospheric new particle formation in China, *Atmos Chem Phys*, 19, 115-138, <https://doi.org/10.5194/acp-19-115-2019>, 2019.
- Kerminen, V. M., Chen, X. M., Vakkari, V., Petäjä, T., Kulmala, M., and Bianchi, F.: Atmospheric new particle formation and growth: review of field observations, *Environ Res Lett*, 13, <https://doi.org/10.1088/1748-9326/aadf3c>, 2018.
- Kontkanen, J., Järvinen, E., Manninen, H. E., Lehtipalo, K., Kangasluoma, J., Decesari, S., Gobbi, G. P., Laaksonen, A., Petäjä, T., and Kulmala, M.: High concentrations of sub-3nm clusters and frequent new particle formation observed in the Po Valley, Italy, during the PEGASOS 2012 campaign, *Atmos Chem Phys*, 16, 17, <https://doi.org/10.5194/acp-16-1919-2016>, 2016.
- Kontkanen, J., Lehtipalo, K., Ahonen, L., Kangasluoma, J., Manninen, H. E., Hakala, J., Rose, C., Sellegri, K., Xiao, S., Wang, L., Qi, X. M., Nie, W., Ding, A. J., Yu, H., Lee, S., Kerminen, V. M., Petaja, T., and Kulmala, M.: Measurements of sub-3nm particles using a particle size magnifier in different environments: from clean mountain top to polluted megacities, *Atmos Chem Phys*, 17, 2163-2187, 2017.
- Kulmala, M., Petäjä, T., Nieminen, T., Sipilä, M., Manninen, H. E., Lehtipalo, K., Dal Maso, M., Aalto, P. P., Junninen, H., Paasonen, P., Riipinen, I., Lehtinen, K. E. J., Laaksonen, A., and Kerminen, V. M.: Measurement of the nucleation of atmospheric aerosol particles, *Nat Protoc*, 7, 1651-1667, <https://doi.org/10.1038/nprot.2012.091>, 2012.
- Kulmala, M., Kontkanen, J., Junninen, H., Lehtipalo, K., Manninen, H. E., Nieminen, T., Petäjä, T., Sipilä, M., Schobesberger, S., Rantala, P., Franchin, A., Jokinen, T., Järvinen, E., Äijälä, M., Kangasluoma, J., Hakala, J., Aalto, P. P., Paasonen, P., Mikkilä, J., Vanhanen, J., Aalto, J., Hakola, H., Makkonen, U., Ruuskanen, T., Mauldin, R. L., Duplissy, J., Vehkamäki, H., Bäck, J., Kortelainen, A., Riipinen, I., Kurtén, T., Johnston, M. V., Smith, J. N., Ehn, M., Mentel, T. F., Lehtinen, K. E. J., Laaksonen, A., Kerminen, V. M., and Worsnop, D. R.: Direct Observations of Atmospheric Aerosol Nucleation, *Science*, 339, 943-946, <https://doi.org/10.1126/science.1227385>, 2013.
- Kulmala, M., Petaja, T., Ehn, M., Thornton, J., Sipila, M., Worsnop, D. R., and Kerminen, V. M.: Chemistry of Atmospheric Nucleation: On the Recent Advances on Precursor Characterization and Atmospheric Cluster Composition in Connection with Atmospheric New Particle Formation, *Annu Rev Phys Chem*, 65, 21-37, 2014.
- Lehtipalo, K., Leppä, J., Kontkanen, J., Kangasluoma, J., Wimmer, D., Franchin, A., Schobesberger, S., Junninen, H., Petäjä, T., Sipilä, M., Mikkilä, J., Vanhanen, J., Worsnop, D. r., and Kulmala, M.: methods for determining particle size distribution and growth rates between 1 and 3 nm using the Particle Size Magnifier, *Boreal Environ Res*, 19, 215-236, 2014.
- Mazon, S. B., Kontkanen, J., Manninen, H. E., Nieminen, T., Kerminen, V.-M., and Kulmala,

M.: A long-term comparison of nighttime cluster events and daytime ion formation in a boreal forest, *Boreal Environment Research*, 21, 19, 2016.

Yao, L., Garmash, O., Bianchi, F., Zheng, J., Yan, C., Kontkanen, J., Junninen, H., Mazon, S. B., Ehn, M., Paasonen, P., Sipilä, M., Wang, M. Y., Wang, X. K., Xiao, S., Chen, H. F., Lu, Y. Q., Zhang, B. W., Wang, D. F., Fu, Q. Y., Geng, F. H., Li, L., Wang, H. L., Qiao, L. P., Yang, X., Chen, J. M., Kerminen, V. M., Petäjä, T., Worsnop, D. R., Kulmala, M., and Wang, L.: Atmospheric new particle formation from sulfuric acid and amines in a Chinese megacity, *Science*, 361, 278-281, <https://doi.org/10.1126/science.aao4839>, 2018.